Morphological evolution of Ge/Si nano-strips driven by Rayleigh-like instability

Marco Salvalaglio,[1,2,a)] Peter Zaumseil,[2] Yuji Yamamoto,[2] Oliver Skibitzki,[2] Roberto Bergamaschini,[3] Thomas Schroeder,[2] Axel Voigt,[1,4] and Giovanni Capellini[2,5]

[1)] *Institute of Scientific Computing, Technische Universität Dresden, 01062 Dresden, Germany*

[2)] *IHP, Im Technologiepark 25, 15236 Frankfurt (Oder), Germany*

[3)] *Department of Materials Science, Università di Milano-Bicocca, Via R. Cozzi 55, I-20126 Milano, Italy*

[4)] *Dresden Center for Computational Materials Science (DCMS), TU Dresden, 01062 Dresden, Germany*

[5)] *Department of Sciences, Università Roma Tre, Viale Marconi 446, I-00146 Roma, Italy*

We present the morphological evolution obtained during the annealing of Ge strips grown on Si ridges as a prototypical process for 3D device architectures and nanophotonic applications. In particular, the morphological transition occurring from Ge/Si nanostrips to nanoislands is illustrated. The combined effect of performing annealing at different temperatures and varying the lateral size of the Si ridge underlying the Ge strips is addressed by means of a synergistic experimental and theoretical analysis. Indeed, three-dimensional phase-field simulations of surface diffusion, including the contributions of both surface and elastic energy, are exploited to understand the outcomes of annealing experiments. The break-up of Ge/Si strips, due to the activation of surface diffusion at high temperature, is found to be mainly driven by surface-energy reduction, thus pointing to a Rayleigh-like instability. The residual strain is found to play a minor role, only inducing local effects at the borders of the islands and an enhancement of the instability.

Semiconductor industry has been able to follow the Moore's law[1] for several decades, providing a continuous increase in functionality and performance per unit chip-area along with a reduction of costs and device switching power. This has been achieved by following standard scaling guidelines[2] and thanks to improvements in fabrication processes such as lithography and patterning. In recent years, consolidated device architectures are missing their performance targets due to the intrinsic limit imposed by their size, thus requiring innovations in materials and new device concepts[3]. Nonplanar, three-dimensional (3D) heterostructures such as FinFETs[4] or gate-all-around, vertical transistors[5] emerged as promising structures to maintain scaling and meet performance requirements[3,6,7]. They also allow for exploiting peculiar features that are absent in bulk-like systems as, e.g., high surface/volume ratios, micro- and nano-strains and composition fluctuations. Moreover, similar nanostructures such as nanowires have been proposed in a wealth of applications in the field of nanophotonics[8,9].

Here we illustrate the evolution during annealing of Ge strips grown on Si ridges, leading to the morphological transition from nanowire-like structures to nanoislands. Indeed, this relatively simple system is prototypical for the study of Ge/Si (or SiGe/Si) FinFET-like structures, e.g. p-channel Ge FinFET, and of most of the newly-developed device architectures[3]. To shed light on this complex evolution, dedicated experiments, continuum modeling and numerical, 3D simulations are presented. In particular, growth and annealing experiments were performed, and the resulting structures were analyzed by X-ray diffraction measurements (XRD). A phase-field (PF) model of surface diffusion[10], tackling the typical physical effects present in heteroepitaxy[11,12] together with the intrinsic three-dimensionality of the system (see recent applications in Refs. 13–18), was exploited to simulate the annealing dynamics. The evolution is shown to result from a diffusion-limited dynamics mainly driven by surface-energy reduction, similarly to what observed in the Rayleigh-Instability[19–21], with specific features related to the interaction with the ridge-like substrate and to the strain after growth.

The most peculiar feature of Ge rods grown on Si ridges is to have an infinite extension in one in-plane direction and limited width along the other. The degree of freedom offered by the width, W, of the Si ridges directly controlled during the fabrication of the substrate, is known to be key in nano-heteroepitaxy[22,23]. Indeed, mismatched structures on islands or vertical substrates with different sizes and Ge content can be adopted to control the elastic relaxation and to hinder, or in general delay, the onset of plasticity[24,25]. In analogy with these studies, we have thus investigated the effect of different widths of the seeding Si ridges on the growth and evolution under annealing of Ge nano-strips.

Si ridges with widths of 95 nm, 55 nm, and 35 nm were realized on 200 mm diameter (001)-oriented SOI wafer. The thickness of the Si ridges is about 30 nm on top of the buried oxide layer[26]. Ge was deposited on Si by a two-step process with a Ge seed layer grown at 300°C, with a thickness of ∼30 nm, followed by the Ge growth process at 550°C[27]. The final epilayer consists of Ge rods

[a)] Electronic mail: marco.salvalaglio@tu-dresden.de

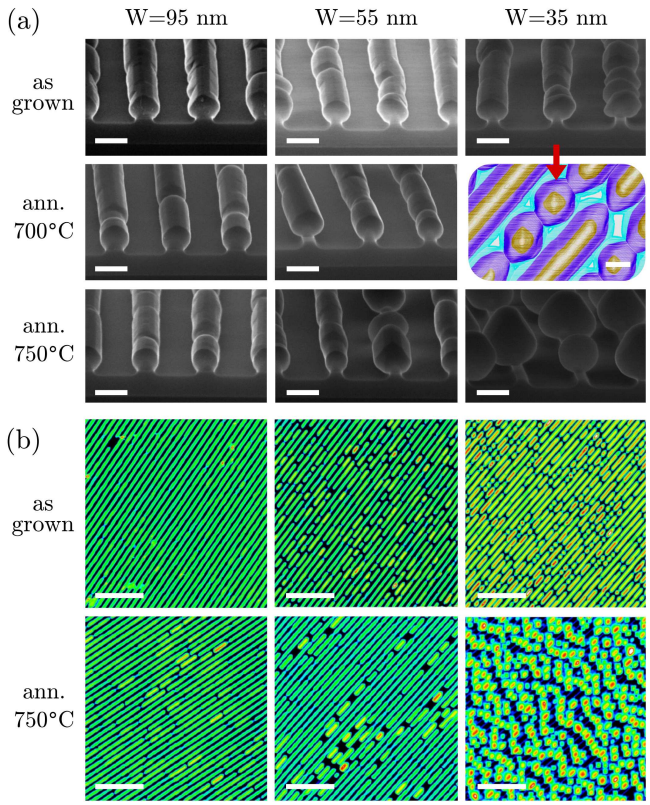

FIG. 1. Morphologies of Ge/Si strips aligned along the [110] direction as grown and after annealing at $T = 700°C$ and $T = 750°C$ for different W. (a) SEM perspective views. White scale bar is 200 nm. A color enhanced AFM scan of the as-grown sample with W=35 nm is also shown (third column, second row). White scale bar is 100 nm. (b) Wide AFM scan of the samples as-grown and annealed at $T = 750°C$. White scale bar is 3 μm.

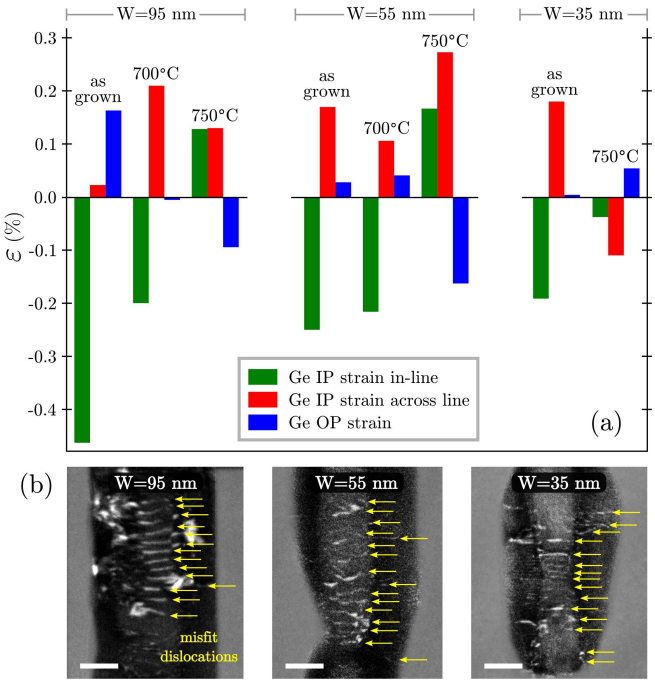

FIG. 2. Strain from XRD measurements and defects at Ge/Si interface. (a) In-plane (IP) strain, in-line and across the strips, as well as out-of-plane (OP) strain are shown for all the samples of Fig. 1. (b) TEM images revealing the presence of dislocations (marked by yellow arrows) in the as-grown structures. White scale bar is 50 nm.

with a radius of $\sim$ 75 nm, independently on W. Different samples were reproduced in order to perform annealing at 700°C and 750°C in H_2 atmosphere for 1 minute.

The morphologies of the resulting structures are illustrated in Fig. 1(a) by SEM images. The first row shows the as-grown Ge/Si strips, for each aforementioned W. Having a size nearly independent of W, Ge rods exhibit different relative contact areas with the underlying Si substrate. Second and third rows illustrate the morphologies obtained after the annealing at 700°C and 750°C, respectively. As can be better observed in the AFM scans of Fig. 1(b), Ge strips tend to breakup with the resulting formation of individual islands. Such a tendency is more pronounced at high temperatures, corresponding to an enhanced diffusivity of thermally-generated adatoms at the surface. Interestingly, the smaller W the more pronounced the breakup of strips occurs. Indeed, for W=35 nm and W=55 nm, a significant fragmentation of the strips is observed already in the as-grown case, while for the largest ridges (W=95 nm) annealing is necessary. For the sample with W=35 nm annealed at 750°C, individual nanoislands are observed, with an average periodicity of $\sim 1.0\mu$m $\pm 0.1\mu$m.

Ge/Si strips are expected to exhibit strain resulting from the lattice mismatch between Ge and Si. However, according to the geometry and sizes considered in this work, also plastic relaxation is expected to occur during growth[23,24]. To get more insight on the structures in Fig. 1, the strain state has been investigated by measurements of strain values averaged over the samples. In particular, XRD measurements in (004) specular diffraction geometry were performed. They allow for the determination of the out-of-plane lattice parameter. Moreover, the in-plane (440) measurement allowed for the determination of the in-plane lattice parameter either along the strips or across them depending on the sample orientation. The averaged in-plain (IP, measured both along and across the strips) and out-of-plane (OP) strain of the Ge rods are reported in Fig. 2(a) for all the samples shown in Fig. 1. They are calculated as the relative difference of the fitted lattice parameters in the corresponding directions with respect to the ones of the relaxed crystal, accounting also for the actual Ge content as a second free parameter which results 95.8% for W=95 nm, 99.4% for W=55 nm, and 100% for W=35 nm (i.e. the epilayers are made of almost pure Ge, with small deviations which can be ascribed to Si in-diffusion in the pedestal region[28]).

In the as-grown samples, the strain along the strips (in-line) is observed to be compressive, featuring values

one order of magnitude smaller than what expected from pure, coherent Ge on Si substrate ($f \sim 0.04$). This points to a strong tendency towards plastic relaxation via the insertion of misfit dislocations. Indeed, such defects are observed in the system as evidenced in Fig. 2(b), showing TEM images of the as-grown structures. Notice that no significant differences were observed among defects distributions in the as-grown samples having different W. The compressive residual strain of Ge along the strips is found to decrease with decreasing W. As the in-line plastic relaxation is nearly the same for all the as-grown samples, this trend can be ascribed to the observed increasing number of free surfaces after the strips breakup (see Fig. 1). Tensile strain is measured across the strips and in the out-of-plane direction as expected from the relaxation given by lateral free surfaces, the Poisson effect due to the uniaxial, compressive deformation along the strips and the thermal strain due to the different expansion coefficients of Ge and Si.

When performing annealing, the motion and elongation of dislocations is generally promoted leading to a higher degree of plastic relaxation with a lowering of the residual strain. Moreover, the strips show higher tendency towards breakup when decreasing W, thus enhancing elastic relaxation (see Fig. 1). In agreement with both these effects, a decrease of the compressive in-line strain is actually obtained for W=95 nm and W=55 nm at 700°C. In the same samples annealed at 750°C, when the motion of dislocations is expected to be further enhanced but still only a few breakups are observed, an almost complete release of misfit strain is achieved. Indeed, a tensile strain even along the strips is measured with a slightly compressive out-of-plane strain, corresponding to the situation observed in fully plastically-relaxed films after thermal treatments. Differently, the annealing at 750°C of the W=35 nm sample leads to isolated islands. The role of free surfaces is here maximized as the breakup is found to occur even during the growth, as shown in Fig. 1. As a result, a residual compressive in-plane strain as well as a tensile out-of-plane strain are observed, resembling what observed in heteroepitaxial islands[29,30]. W is then found to affect how fast the strips break and the further relaxation of the residual strain after growth.

In order to assess the role of W and to shed light on the main mechanism at play during the morphological evolution, we have carried out a theoretical analysis of the system. Elongated structures are expected to breakup because of the Rayleigh instability driven by capillarity[19–21]. In particular, a solid cylinder with isotropic surface energy is expected to be unstable for perturbations of the surface with a wavelength larger than $\lambda_c = 2\pi R$, with R the radius of the cylinder, featuring a most unstable wavelength of $\lambda_{max} = \sqrt{2}\lambda_c$. When accounting for elongated structures in contact with a planar substrate, these values are known to increase, depending on the contact angle[31,32]. For instance, the most unstable wavelength of a half cylinder having a contact angle with the substrate of 90° is[31] $\lambda^{90}_{max} \sim 8\pi R\sqrt{2/3}$. The Ge/Si strips considered in this work are actually in contact with a non-planar substrate. The periodicity observed in our experiments is in between the ones expected for these two limiting cases, $\lambda_{max} = 667$ nm and $\lambda^{90}_{max} \sim 1540$ nm, calculated for the measured radius $R = 75$ nm. In principle, to better describe the real system, two additional aspects have to be considered. One is the faceting of the Ge crystals (evident in the AFM view of Fig. 1(a)), reflecting anisotropies in the surface energy, that may alter the unstable wavelength as found in metals[33]. The other is the Ge/Si misfit strain resulting in an additional contribution to the chemical potential favoring diffusion in the direction toward strain minimization (see the ATG instability[34–36]). In the present work, we focused on this latter contribution while retaining a fully isotropic surface energy density for the sake of simplicity.

To address the specific case of the Ge strips on Si ridges shown in Fig. 1, accounting also for different values of W, we focused on the modeling of thermally-activated material transport at their surface[37] by means of a PF model of surface diffusion as illustrated in detail in the Supplementary Material. In brief, an order parameter $\varphi(\mathbf{x})$ was considered, that is $\varphi = 1$ in the solid phase, $\varphi = 0$ in the vacuum phase with a continuous variation over an interface region with thickness ϵ. The evolution law for φ reproducing surface diffusion is given by the degenerate Cahn-Hilliard model[10]. Both surface energy and elastic relaxation as introduced in Ref. 38 were considered. The former accounts for the isotropic surface-energy density γ and for the extension of the surface. The latter accounts for the deformations of the system due to the mismatch between the lattice-parameter a of the epilayer and the substrate $\varepsilon_m = (a_{sub} - a_{epi})/a_{epi}$, for the elastic relaxation given by free surfaces and for compliance effects of the substrate. In particular, we assumed to have a hydrostatic strain with $\varepsilon_m = -0.005$, as suggested by XRD measurements. An additional composition field c, as adopted in Refs. 16 and 39, was also considered to account in detail for the presence of a substrate and Ge/Si material properties. PF simulations were performed by using the Finite Element Method (FEM) toolbox AMDiS[40,41] with time adaptivity and mesh refinement at the solid-vacuum interface. Further details about simulations are reported in the Supplementary Material.

First we focused on a prescribed, small perturbation of the Ge strip, set by considering a sinusoidal variation of the radius $r = R + \delta\cos(2\pi x/\lambda)$, with x the coordinate along the strip, and $R = 75$ nm as in the experiments. From Fig. 1 we extracted $\lambda^{exp}_{max} = 1\mu$m, and we then expect to have a $\lambda^{exp}_c \approx \lambda^{exp}_{max}/\sqrt{2} = 710$ nm. We then selected $\lambda = 750$ nm, that is slightly larger than λ^{exp}_c to verify the consistency with the standard Rayleigh instability. δ set the magnitude of the small perturbation with δ=$\epsilon/2$=5 nm. The modeling of the structure by PF is reported in Fig. 3(a). Cross-sections of the initial profile for different W values are illustrated in Fig. 3(b). Actually, the structure with W=35 nm is unstable. This is

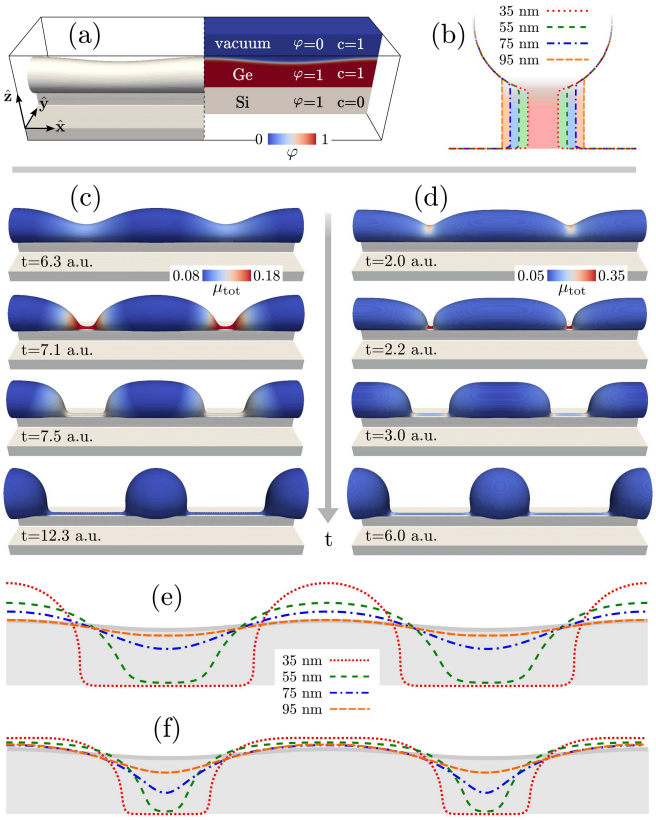

FIG. 3. Evolution of a Ge strip on a Si ridge by PF simulations. (a) Initial morphology. Surface of the solid phase (left), namely $\varphi = 0.5$, and an in-line cross section showing the modeling of materials (right) are shown. (b) Change in the morphology with different W. (c) and (d) Morphological evolution of the structure in panel (a) without strain and with $\varepsilon_m = -0.005$, respectively. (e) and (f) Comparison of profiles for different W at $t = 10$ a.u without strain and at $t = 3$ a.u. with $\varepsilon_m = -0.005$, respectively. Light gray areas in the background of panel (e) and (f) correspond to the Ge domain of the initial geometry.

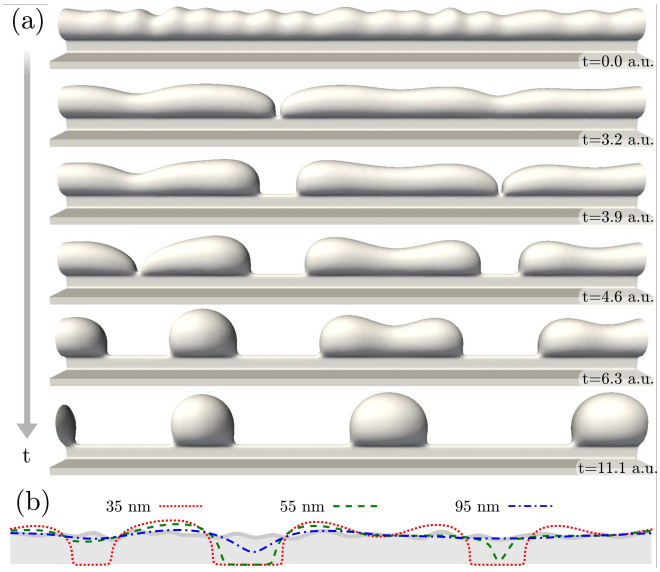

FIG. 4. PF Simulations of Ge/Si strips starting from an initial random profile and $\varepsilon_m = -0.005$. (a) Representative steps of the evolution with W=35 nm. (b) Comparison of the surface profiles at t=5 a.u. obtained with an initial Ge morphology as in panel (a) and different W.

shown by the PF simulation in Fig. 3(c), where only the contribution of surface energy was considered. An amplification of the initial perturbation is achieved in the first stages followed by the breakup when the surface of the Ge strip reaches the Si ridge. Eventually, isolated islands form, qualitatively reproducing the outcome of the experiments in Fig. 1. It is worth mentioning that a perturbation with $\lambda = 500$ nm, slightly larger than the critical wavelength for classical Rayleigh instability $\lambda_c \sim 470$ nm, is stable, thus confirming the effect of the interaction with the substrate[31,32]. The additional effect of elastic energy reduction due to the residual strain as in the experiments ($\varepsilon_m = -0.005$) is shown in Fig. 3(d). In a shorter time scale, localized trenches develop until touching the substrate. Then, they widen until the formation of isolated islands. Overall, the outcome of this evolution closely resembles the one without strain in Fig. 3(c), except for the formation of localized trenches that trigger the breakup process on a shorter timescale.

The role of W was addressed with and without the residual strain as shown in Figs. 3(e) and 3(f), respectively. Without strain, a delay is observed when increasing W as shown by the surface profiles along the Ge strips at $t = 10$ a.u. in Fig. 3(e). This is compatible with the results of Refs. 31 and 32 where the interaction of a wire with the substrate is proved to increase its stability. As known from studies of confined structures[24], by increasing the lateral size of the Ge/Si interface a worse elastic relaxation of the misfit strain is expected, thus leading to a larger contribution of elasticity to the chemical potential at the surface. However, when considering the sizes and the strain of the experiments reported here, as illustrated in Fig. 3(f) at $t = 3$ a.u., a similar trend as in Fig. 3(e) is obtained, with a relative delay in the evolution that is decreased with respect to the case without strain. Thus, the delay in the breakup with increasing W as observed in Fig. 1 is reproduced by the model, that demonstrates the major role played by a Rayleigh-like instability and by the extension of the Ge/Si interface. Elasticity effects are found to give only minor contributions due to the low values of residual strain in the sample, i.e. due to the high degree of plastic relaxation. Notice that, also the effect of the temperature as in Fig. 1 is included in the model. Indeed, the higher T, the larger D values are (see Supplementary Material), thus producing a faster evolution and, in turn, an earlier instability onset.

A closer examination of the experimental case was performed by considering a surface profile given by a random modulation of r on a larger system with a total length of

3 μm (as the scale bar in Fig. 1(b)). For the sake of generality we included both surface- and elastic-energy contributions, the latter set as in the simulation of Fig. 3(d). The PF simulations match well with the results of the experiments in Fig. 1. Indeed, as shown in Fig. 4(a) where W=35 nm, after a first fast smoothing of the initial profile, the strip breaks at different points and times, eventually forming isolated islands. An average spacing of $\sim 1\mu$m is obtained, that is compatible with the experimental observations. The good agreement with the wavelength of the experiments suggests that also anisotropy of the surface-energy density, not included in the simulations, plays a minor role in the observed morphological evolution. The delay in the onset of the instability and in the formation of islands with increasing W was reproduced also for randomly perturbed profiles as illustrated in Fig. 4(b). This figure shows the corresponding in-line surface profile of the Ge rods at $t = 5$ a.u. obtained with different W with an initial random perturbation of the epilayer as in Fig. 4(a).

In conclusion, we outlined the unstable nature of Ge/Si strips, characterized their strain and explained their morphological evolution. A fast dynamics is obtained for narrow Si ridges, while it slows down by increasing the width of the Si ridges. This difference is found to affect the relaxation mechanisms of the misfit strain. In any case, when annealed at high temperature for long times, Ge/Si strips may result unsuitable for channel-like devices as they would evolve towards the formation of self-assembled clusters. PF simulations revealed the main mechanism at play during high-temperature treatments promoting surface diffusion. It consists in the reduction of surface-energy, leading to a Rayleigh-like instability, influenced by the interaction with the substrate. The effect of elastic energy reduction is found to play a minor role due to the low residual-strain values measured in the system, only slightly affecting the morphologies during the break-up of stripes and the timescale of the process. Future work will be devoted to the investigation of similar behaviors in systems having larger strains.

See the Supplementary Material for the details about the phase-field modeling.

We acknowledge R. Backofen (TU-Dresden) for fruitful discussions and M. A. Schubert (IHP) for TEM measurements. M.S. acknowledges the support of the Postdoctoral Research Fellowship awarded by the Alexander von Humboldt Foundation. The computational resources were provided by ZIH at TU-Dresden and by the Jülich Supercomputing Center within the Project No. HDR06.

[1] G. E. Moore, Electronics **38**, 114 (1965).
[2] R. Dennard, F. Gaensslen, V. Rideout, E. Bassous, and A. LeBlanc, IEEE J. Solid-St. Circ. **9**, 256 (1974).
[3] N. Collaert, A. Alian, H. Arimura, G. Boccardi, G. Eneman, J. Franco, T. Ivanov, D. Lin, R. Loo, C. Merckling, *et al.*, Microelectronic Eng. **132**, 218 (2015).
[4] X. Huang, W. C. Lee, C. Kuo, D. Hisamoto, L. Chang, J. Kedzierski, E. Anderson, H. Takeuchi, Y. K. Choi, K. Asano, *et al.*, IEEE T. Electron Dev. **48**, 880 (2001).
[5] N. Singh, A. Agarwal, L. Bera, T. Liow, R. Yang, S. Rustagi, C. Tung, R. Kumar, G. Lo, N. Balasubramanian, *et al.*, IEEE Electr. Device L. **27**, 383 (2006).
[6] A.-Y. Thean, N. Collaert, I. P. Radu, N. Waldron, C. Merckling, L. Witters, R. Loo, J. Mitard, R. Rooyackers, A. Vandooren, *et al.*, ECS Transactions **66**, 3 (2015).
[7] R. Loo, A. Y. Hikavyy, L. Witters, A. Schulze, H. Arimura, D. Cott, J. Mitard, C. Porret, H. Mertens, P. Ryan, *et al.*, ECS Transactions **75**, 491 (2016).
[8] C. P. T. Svensson, T. Martensson, J. Trägardh, C. Larsson, M. Rask, D. Hessman, L. Samuelson, and J. Ohlsson, Nanotechnology **19**, 305201 (2008).
[9] R. Yan, D. Gargas, and P. Yang, Nat Photonics **3**, 569 (2009).
[10] B. Li, J. Lowengrub, A. Ratz, and A. Voigt, Commun. Comput. Phys. **6**, 433 (2009).
[11] Y. Tu and J. Tersoff, Phys. Rev. Lett. **98**, 096103 (2007).
[12] R. Bergamaschini, M. Salvalaglio, R. Backofen, A. Voigt, and F. Montalenti, Adv. Phys. X **1**, 331 (2016).
[13] M. Salvalaglio, R. Bergamaschini, F. Isa, A. Scaccabarozzi, G. Isella, R. Backofen, A. Voigt, F. Montalenti, G. Capellini, T. Schroeder, *et al.*, ACS Appl. Mat. Interfaces **7**, 19219 (2015).
[14] M. Salvalaglio, R. Backofen, R. Bergamaschini, F. Montalenti, and A. Voigt, Cryst. Growth Des. **15**, 2787 (2015).
[15] M. Salvalaglio, R. Backofen, and A. Voigt, Phys. Rev. B **94**, 235432 (2016).
[16] M. Albani, R. Bergamaschini, and F. Montalenti, Phys. Rev. B **94**, 075303 (2016).
[17] M. Salvalaglio, R. Backofen, A. Voigt, and F. Montalenti, Nanoscale Res. Lett. **12**, 554 (2017).
[18] M. Naffouti, R. Backofen, M. Salvalaglio, T. Bottein, M. Lodari, A. Voigt, T. David, A. Benkouider, I. Fraj, L. Favre, *et al.*, Sci. Adv. **3**, eaao1472 (2017).
[19] L. Rayleigh, P. Lond. Math. Soc. **s1-10**, 4 (1878).
[20] F. A. Nichols and W. W. Mullins, J. Appl. Phys. **36**, 1826 (1965).
[21] D. J. Srolovitz and S. A. Safran, J. Appl. Phys. **60**, 247 (1986).
[22] D. Zubia and S. D. Hersee, J. Appl. Phys. **85**, 6492 (1999).
[23] F. Montalenti, M. Salvalaglio, A. Marzegalli, P. Zaumseil, G. Capellini, T. U. Schülli, M. A. Schubert, Y. Yamamoto, B. Tillack, and T. Schroeder, Phys. Rev. B **89**, 014101 (2014).
[24] M. Salvalaglio and F. Montalenti, J. Appl. Phys. **116**, 104306 (2014).
[25] F. Isa, M. Salvalaglio, Y. A. R. Dasilva, M. Medua, M. Barget, A. Jung, T. Kreiliger, G. Isella, R. Erni, F. Pezzoli, *et al.*, Adv. Mater. **28**, 884 (2016).
[26] P. Zaumseil, G. Kozlowski, Y. Yamamoto, J. Bauer, M. a. Schubert, T. U. Schülli, B. Tillack, and T. Schroeder, J. Appl. Phys. **112**, 043506 (2012).
[27] Y. Yamamoto, K. Köpke, R. Kurps, J. Murota, and B. Tillack, Thin Solid Films **518**, S44 (2010).
[28] G. Niu, G. Capellini, G. Lupina, T. Niermann, M. Salvalaglio, A. Marzegalli, M. A. Schubert, P. Zaumseil, H.-M. Krause, O. Skibitzki, *et al.*, ACS Appl. Mater. Interfaces **8**, 2017 (2016).
[29] V. Shchukin and D. Bimberg, *Rev. Mod. Phys.*, **71**, 1125 (1999).
[30] J. Stangl, V. Holý, and G. Bauer, *Rev. Mod. Phys.*, **76**, 725 (2004).
[31] M. S. McCallum, P. W. Voorhees, M. J. Miksis, S. H. Davis, and H. Wong, J.Appl. Phys. **79**, 7604 (1996).
[32] S. P. A. Gill, Appl. Phys. Lett. **102** (2013).
[33] G. H. Kim and C. V. Thompson, Acta Materi. **84**, 190 (2015).
[34] R. J. Asaro and W. A. Tiller, Metall. Trans. , 1789 (1972).
[35] D. Srolovitz, Acta Metall. **37**, 621 (1989).
[36] M. A. Grinfeld, J. Nonlinear Sci. **3**, 35 (1993).
[37] W. W. Mullins, J. Appl. Phys. **28**, 333 (1957).
[38] A. Rätz, A. Ribalta, and A. Voigt, J. Comput. Phys. **214**, 187 (2006).
[39] S. M. Wise, J. S. Lowengrub, J. S. Kim, K. Thornton, P. W. Voorhees, and W. C. Johnson, Appl. Phys. Lett. **87**, 133102 (2005).
[40] S. Vey and A. Voigt, *Comput. Visual. Sci.*, **10**, 57 (2007).
[41] T. Witkowski, S. Ling, S. Praetorius, and A. Voigt, Adv. Comput. Math. **41**, 1145 (2015).